

Optimal Nonnegative Color Scanning Filters

Gaurav Sharma*

H. Joel Trussell[†]

Michael J. Vrhel[‡]

Abstract

In this correspondence, the problem of designing color scanning filters for multi-illuminant color recording is considered. The filter transmittances are determined from a minimum-mean-squared orthogonal tristimulus error criterion, that minimizes the color error in estimates obtained from noisy recorded data. Non-negativity constraints essential for physical realizability are imposed on the filter transmittances. In order to demonstrate the significant improvements obtained, the resulting filters are compared with sub-optimal filters reported in earlier literature.

1 Introduction

It is well known that the color of an object is dependent upon the illuminant under which it is viewed. In certain applications, the color of an object under several different viewing-illuminants must be estimated from measurements obtained with a single device. Examples of such applications include paint and textile industries, where it is desirable to monitor and minimize the color variation of paint/dye lots under common home, office, and daylight illumination, and computer graphics simulations, where a single scene may need to be rendered under several different lighting conditions.

The problem of accurately recovering color information under multiple viewing-illuminants can be posed as a color-filter design problem. Reference [1] described a method of computing transmittances of filters that minimized the minimum-mean-squared tristimulus error. The design of color recording filters for a device capable of both reflective and emissive measurements has also been described recently by Wolski *et al.* [2]. Their method minimizes mean-squared error (MSE) in a linearized perceptually-uniform color space. Regularization terms are used to enforce smoothness on the designed transmittances and to provide robustness in the presence of noise and component variations in the filters. Since noise was not explicitly included in the analysis, the weighting of the regularization term was determined empirically.

Ref. [3] addressed the specific problem of designing color filters which account for the presence of noise in the recording process. The approach used a minimum-mean-squared orthogonal-tristimulus error formulation. Closed-form solutions for optimal scanning filters at various signal-to-noise ratios (SNRs) were determined,

*Xerox Corporation, MS0128-27E, 800 Phillips Rd, Webster, NY 14580. Email: sharma@wrc.xerox.com. This work was done while G. Sharma was at NCSU.

[†]ECE Dept., North Carolina State University, Raleigh, NC 27695-7911. Email: hjt@eos.ncsu.edu.

[‡]National Institutes of Health, Bethesda, MD 20892. Email: vrhel@helix.nih.gov

and the relation of the number of filters to the color error was examined. However, the closed-form solutions were not constrained to be nonnegative, which is necessary for physical feasibility. A constrained version of the problem requiring the filters to be nonnegative was also formulated, but since the problem had a nonlinear power constraint, only a sub-optimal solution to that problem was obtained based on the unconstrained solution. In this correspondence, the same constrained problem is considered. Through a simple modification, the problem is transformed to one having only nonnegativity constraints. A numerical optimization scheme is utilized to determine the optimal solution. Results indicate significant improvement over the previous sub-optimal solution.

2 Problem Formulation

For completeness, the problem formulation from [3] will be briefly summarized. Typically, color scanners filter the reflected light from the scanned object into spectral-bands and record the light energy in each band using radiation detectors. The spectra will be represented here by N -component vectors, consisting of equi-spaced samples in the visible region from 400 to 700 nm. If a K channel scanner is used, the measurement of an object whose reflectance is specified by the N -vector \mathbf{r} can be algebraically represented as [3, 4]

$$\mathbf{t}_s = \mathbf{M}^T \mathbf{L}_s \mathbf{r} + \boldsymbol{\eta} = \mathbf{G}^T \mathbf{r} + \boldsymbol{\eta}, \quad (1)$$

where \mathbf{t}_s is a $K \times 1$ vector of scanner measurements, \mathbf{L}_s is the $N \times N$ diagonal matrix with samples of the scanner-illuminant spectrum along the diagonal, $\boldsymbol{\eta}$ is the $K \times 1$ measurement noise vector, $\mathbf{G} = \mathbf{L}_s \mathbf{M}$, and $\mathbf{M} = [\mathbf{m}_1, \mathbf{m}_2, \dots, \mathbf{m}_K]$ is the $N \times K$ matrix of scanner filter transmittances, where \mathbf{m}_i represents the spectral transmittance of the i th filter (including detector sensitivity and the transmittance of the scanner optical path).

The color of an object, under a given viewing illuminant, is specified by its CIE XYZ tristimulus value [5]. If there are J viewing illuminants, in a manner analogous to the scanner measurements, the tristimuli of the object with spectral reflectance, \mathbf{r} , can be written as [4, 3]

$$\mathbf{t}_i = \mathbf{A}^T \mathbf{L}_i \mathbf{r} = \mathbf{A}_{\mathbf{L}_i}^T \mathbf{r}, \quad i = 1, 2, \dots, J; \quad (2)$$

where \mathbf{t}_i is the 3×1 vector of CIE XYZ tristimulus values under the i^{th} viewing-illuminant, \mathbf{A} is the $N \times 3$ matrix of CIE XYZ color-matching functions [5], \mathbf{L}_i is the $N \times N$ diagonal matrix with samples of the i^{th} viewing-illuminant spectrum along the diagonal, and $\mathbf{A}_{\mathbf{L}_i} = \mathbf{L}_i \mathbf{A}$.

Colorimetric information about the object is determined from the scanner measurements by estimating the tristimulus values. The scanning-filter design problem can be formulated as a problem of minimizing the MSE

in estimated CIE tristimuli. Such a procedure suffers from two drawbacks: the CIE XYZ tristimulus values are highly correlated, and significant magnitude differences can exist between different illuminants. Hence, as in [3], each of the illuminant color-matching matrices, $\{\mathbf{L}_i \mathbf{A}\}_{i=1}^J$, is orthonormalized to obtain $\{\mathbf{O}_i\}_{i=1}^J$, such that \mathbf{O}_i has orthonormal columns and a range space identical to that of $\mathbf{L}_i \mathbf{A}$. The vector $\mathbf{O}_i^T \mathbf{r}$ then represents a tristimulus in an orthogonal tristimulus space. Note that the magnitude differences between illuminants could also be eliminated through simple scaling. However, the orthonormalization procedure is preferred because in comparison with mean-squared errors in the highly correlated CIEXYZ space, those in the orthonormalized tristimulus space correlate better with perceptual measures of color difference [6].

The problem of scanner design is now formulated as an optimization problem, where the color filter/recording illuminant matrix, \mathbf{G} , is chosen so as to minimize the MSE in the orthogonal tristimulus space,

$$\epsilon = \sum_{i=1}^K \gamma_i^2 E\{||\mathcal{P}_i(\mathbf{t}_s) - \mathbf{O}_i^T \mathbf{r}||^2\}, \quad (3)$$

where $\mathcal{P}_i(\cdot)$ is an illumination color-correction transformation for the i th illuminant, which estimates the tristimuli $\mathbf{O}_i^T \mathbf{r}$ from the scanner measurements \mathbf{t}_s ; the γ_i^2 are used to provide a weighting for the cost of color errors under the various illuminants; and E denotes the expectation operator (taken over the reflectance spectra and the additive noise).

If the noise $\boldsymbol{\eta}$ is assumed to be uncorrelated with the signal $\mathbf{G}^T \mathbf{r}$, then it can be seen that the linear minimum MSE (LMMSE) estimator of the orthogonal tristimuli is

$$\mathcal{P}_i(\mathbf{t}_s) = \mathbf{O}_i^T \mathbf{K}_r \mathbf{G} \left[\mathbf{G}^T \mathbf{K}_r \mathbf{G} + \mathbf{K}_\eta \right]^{-1} \left[\mathbf{t}_s - \bar{\boldsymbol{\eta}} - \mathbf{G}^T \bar{\mathbf{r}} \right] + \mathbf{O}_i^T \bar{\mathbf{r}} \quad (4)$$

where \mathbf{K}_r is the covariance matrix of the reflectance spectra, \mathbf{K}_η is the covariance matrix of the noise, $\bar{\mathbf{r}}$ is the mean of the reflectance spectra, and $\bar{\boldsymbol{\eta}}$ is the mean of the noise [7]. In this work, only linear illumination color-correction transformations ($\mathcal{P}_i(\cdot)$) are considered. Alternate higher-order polynomial transformations are not explored due to the mathematical intractability of the resulting problem, and because higher order polynomials offer insignificant gains over a linear transformation when the input is not constrained to a restricted class [8].

Substituting (4) in (3), it can be readily seen that the LMMSE can be written as $\epsilon_{LMMSE} = \alpha - \tau(\mathbf{G})$, where $\alpha = \text{tr}(\mathbf{S} \mathbf{S}^T \mathbf{K}_r)$ and

$$\tau(\mathbf{G}) = \text{tr} \left(\mathbf{S} \mathbf{S}^T \mathbf{K}_r \mathbf{G} \left[\mathbf{G}^T \mathbf{K}_r \mathbf{G} + \mathbf{K}_\eta \right]^{-1} \mathbf{G}^T \mathbf{K}_r \right), \quad (5)$$

where $\mathbf{S} = [\gamma_1 \mathbf{O}_1, \gamma_2 \mathbf{O}_2, \dots, \gamma_J \mathbf{O}_J]$ and $\text{tr}(\cdot)$ denotes the trace operator. Since the sensor measurements are performed independently on the K channels, it will be assumed that $\mathbf{K}_\eta = \sigma^2 \mathbf{I}$, where σ^2 denotes the variance of the noise in the individual measurement channels.

It is clear that ϵ_{LMMSE} is minimized if the filter/illuminant matrix \mathbf{G} is chosen so as to maximize $\tau(\mathbf{G})$. In practice, the recording device is subject to additional limitations of illuminant intensity and integration

time. In order to incorporate these, it is assumed, as in [3], that the expectation of the total signal power is constrained to be a finite positive number, ρ . Mathematically, this assumption is stated as $E\{\|\mathbf{G}^T \mathbf{r}\|^2\} = \rho$.

Note that with this constraint on the signal power, the problem of selecting the optimal nonnegative filter/illuminant matrix, \mathbf{G} , can be stated as [3]

$$\max_{\mathbf{G}} \tau(\mathbf{G}) \quad \text{subject to} \quad \mathbf{G}^T \geq \mathbf{0}, \quad \text{tr}(\mathbf{G}^T \mathbf{K}_r \mathbf{G}) = \kappa, \quad (6)$$

where $\kappa = \rho - \|\mathbf{G} \bar{\mathbf{r}}\|^2$.

This problem was formulated in Ref. [3], where it was stated that the problem is difficult to solve due to the nonlinear signal power constraint. A suboptimal solution was determined in [3] through a two step process, first optimal filter sets that were not constrained to be nonnegative were determined analytically, and then nonnegative filters that approximate the unconstrained optimal filters were obtained through a numerical optimization procedure. In the next section, it will be shown that a simple modification of the problem eliminates the nonlinear constraint, allowing the problem to be solved directly.

3 Constraint Simplification

In practice, the parameters, κ and σ^2 , in the above optimization problem are not known in absolute terms. Instead, their ratio κ/σ^2 , defined as the SNR, is usually estimated from a knowledge of the detector noise characteristics and the device quantization requirements. Therefore, problem (6) is more completely stated as

$$\max_{\mathbf{G}} \tau(\mathbf{G}) \quad \text{subject to} \quad \mathbf{G}^T \geq \mathbf{0}, \quad \text{tr}(\mathbf{G}^T \mathbf{K}_r \mathbf{G}) = \kappa, \quad \frac{\kappa}{\sigma^2} = \Gamma, \quad (7)$$

where Γ is the SNR.

By eliminating σ^2 , (7) can be rewritten as

$$\max_{\mathbf{G}} f(\mathbf{G}) \equiv \text{tr} \left(\mathbf{S} \mathbf{S}^T \mathbf{K}_r \mathbf{G} \left[\mathbf{G}^T \mathbf{K}_r \mathbf{G} + \frac{\text{tr}(\mathbf{G}^T \mathbf{K}_r \mathbf{G})}{\Gamma} \mathbf{I} \right]^{-1} \mathbf{G}^T \mathbf{K}_r \right) \quad (8)$$

subject to $\mathbf{G}^T \geq \mathbf{0}$, $\text{tr}(\mathbf{G}^T \mathbf{K}_r \mathbf{G}) = \kappa$.

Note that the objective function is invariant to a scaling of \mathbf{G} . Hence, if the solution to this problem is denoted as $\mathbf{G}_{opt}(\kappa, \Gamma)$ then the solution to the corresponding problem where the signal power is scaled by a positive constant α is simply $\mathbf{G}_{opt}(\alpha\kappa, \Gamma) = \sqrt{\alpha} \mathbf{G}_{opt}(\kappa, \Gamma)$. Hence, given a solution to the problem

$$\max_{\mathbf{G}} f(\mathbf{G}) \quad \text{subject to} \quad \mathbf{G}^T \geq \mathbf{0}, \quad (9)$$

the solution to problem (7) can be immediately found by scaling with a positive scalar to satisfy the constraint $\text{tr}(\mathbf{G}^T \mathbf{K}_r \mathbf{G}) = \kappa$.

Since (9) involves only a nonnegativity constraint, it is more readily handled by numerical optimization programs than the optimization in (6), which involved an additional nonlinear constraint. Even a small amount of noise ensures that the function, $f(\cdot)$, is differentiable everywhere with gradient $\frac{\partial f}{\partial \mathbf{G}}$, given by [9]

$$\begin{aligned} \frac{1}{2} \frac{\partial f}{\partial \mathbf{G}} = & \mathbf{K}_r \mathbf{S} \mathbf{S}^T \mathbf{K}_r \mathbf{G} \left[\mathbf{G}^T \mathbf{K}_r \mathbf{G} + \frac{\text{tr}(\mathbf{G}^T \mathbf{K}_r \mathbf{G})}{\Gamma} \mathbf{I} \right]^{-1} + \\ & \mathbf{K}_r \mathbf{G} \left[\mathbf{G}^T \mathbf{K}_r \mathbf{G} + \frac{\text{tr}(\mathbf{G}^T \mathbf{K}_r \mathbf{G})}{\Gamma} \mathbf{I} \right]^{-1} \mathbf{G}^T \mathbf{K}_r \mathbf{S} \mathbf{S}^T \mathbf{K}_r \mathbf{G} \left[\mathbf{G}^T \mathbf{K}_r \mathbf{G} + \frac{\text{tr}(\mathbf{G}^T \mathbf{K}_r \mathbf{G})}{\Gamma} \mathbf{I} \right]^{-1} + \\ & \frac{1}{\Gamma} \text{tr} \left(\mathbf{K}_r \mathbf{S} \mathbf{S}^T \mathbf{K}_r \mathbf{G} \left[\mathbf{G}^T \mathbf{K}_r \mathbf{G} + \frac{\text{tr}(\mathbf{G}^T \mathbf{K}_r \mathbf{G})}{\Gamma} \mathbf{I} \right]^{-2} \right) \mathbf{K}_r \mathbf{G}. \end{aligned} \quad (10)$$

If the covariance matrix of the reflectance spectra and the parameters of the scanning illuminant in \mathbf{S} are known, the expressions for the function and the gradient can be readily used in gradient-projection optimization schemes [10] to determine the (locally) optimal solution to (9).

4 Experimental Results and Discussion

The multi-illuminant color recording problem simulated in [3] was used to evaluate the usefulness of the new procedure (which determines the optimal solution to (6)) in comparison to the sub-optimal solution proposed in [3]. A sampling width of 10nm was used, which resulted in $N = 31$ samples between 400 and 700 nm. A reflectance spectra ensemble, consisting of 343 spectral reflectances from a color copier, was used to determine the spectral covariance, \mathbf{K}_r ¹. The CIE incandescent illuminant A, CIE daylight illuminant D65, and CIE fluorescent illuminant F2, were used as the viewing illuminants, with unity weighting factors (γ_i), to determine the matrix \mathbf{S} . Using a commercial scientific-optimization routine [11] based on a modified-Newton method with gradient-projection, sets of 3 to 7 color filters were calculated for SNRs of 30, 35, 40, 45, and 50 dB.

Some comments about the numerical behavior of the optimization problem (9) would be appropriate here. As mentioned earlier the objective function, $f(\mathbf{G})$, is invariant under scalar transformations of \mathbf{G} . Therefore, the problem does not have a unique solution, and every positive scalar multiple of a maximizer is also a maximizer. This leads to undesirable scaling problems in the vicinity of $\mathbf{G} = \mathbf{0}$. For numerical stability and improved convergence, it is desirable to have a (locally) unique solution. Therefore, one of the elements of \mathbf{G} was constrained to be unity. For most cases, the sub-optimal solutions from [3] were used as initial starting points for the iterative optimization routines and the maximum element in the initialization was constrained to be unity. Experimentation with alternate initial points revealed that the solution was not unduly sensitive to the initialization in the cases examined, and the unity constraint did not create any problem as long as it was

¹Results for other ensembles of reflectance spectra were similar to those of the copier data set.

applied to an arbitrary element in the green region of the spectrum (approx. 500 to 550 nm). The algorithm converged fairly fast, requiring under 20 iterations in most cases.

The matrix \mathbf{G} in (1) represents the combination of the recording-illuminant and the transmittances/sensitivities of the filters and other components in the scanner. For brevity, in the following discussion, it will be referred to as the scanning filter-set and its elements will be called filter transmittances. The solution to (9) obtained by the above procedure will therefore be alluded to as the optimal (nonnegative) filter-set, and the nonnegative solution from [3] will be called the sub-optimal filter-set.

Using simulations, the recording accuracy of the optimal filter-sets obtained from the above procedure was compared with the accuracy of the sub-optimal filter-sets of [3]. In order to perform the comparison, for each filter-set (optimal/sub-optimal and having between 3 and 7 filters) a noisy recording of the copier data-set used in [3] was simulated using the model of (1), where white Gaussian noise, with variance determined by the SNR, was used for $\boldsymbol{\eta}$. The CIE tristimulus vectors of the spectral reflectance samples under the three viewing illuminants were estimated from the recorded data using an LMMSE estimator (Eq. (4) with \mathbf{O}_i replaced by $\mathbf{A}_{\mathbf{L}_i}$). True tristimuli were also calculated using (2). In order to calculate color errors in perceptually relevant units, the tristimuli were converted to CIE $L^*a^*b^*$ space [5, 12] and the ΔE_{ab}^* error (Euclidean distance in $L^*a^*b^*$ space) was computed for each estimated tristimulus. For each filter set, average ΔE_{ab}^* errors were computed over the copier reflectance-ensemble and the viewing illuminants. The average ΔE_{ab}^* errors for the optimal and the sub-optimal filter sets are compared in Fig. 1, for SNRs of 30, 40, and 50 dB. The number of filters is represented along the abscissa and the average ΔE_{ab}^* errors are plotted along the ordinate for different filter-sets, with the crosses (\times) representing averages for the sub-optimal filters from [3], and the circles (o) representing the averages for the optimal filters obtained by the aforementioned procedure. The number of filters is integral, but lines joining the points have been plotted to facilitate comparison and comments.

Several interesting observations can be made from Fig. 1. First observe that the optimal filters perform consistently better than the sub-optimal filters. Given the nonlinear relation of the CIE $L^*a^*b^*$ space to the orthogonal-tristimulus space in which the optimal filters are defined, this improvement does not directly follow from the “optimality”. The reduction in error is significant for all filter-sets, but the largest improvements in average ΔE_{ab}^* performance are at low SNRs and for filter sets with large number of filters. Intuitively, one expects the average error to monotonically decrease as additional filters are added at a given SNR. The optimal filters follow this trend, but due to the additional constraints on the sub-optimal filters, they often show an increase in average ΔE_{ab}^* error with increase in the number of filters. These facts indicate that the additional constraints imposed on the filters in defining the sub-optimal solution were inappropriate. One may also note here that in the absence of noise, $f(\mathbf{G})$ is invariant under nonsingular transformations of \mathbf{G} [13]. Therefore, in the absence of noise, nonnegative filters can be obtained by a nonsingular transformation of the optimal

unconstrained filters [14]. Since the sub-optimal filters were initialized using such nonsingular transformations, this fact explains the (relative) improvement in performance of the sub-optimal filter-sets at high SNR's.

A more complete summary of the ΔE_{ab}^* error statistics for the optimal filters appears in Table 1. For each SNR, viewing-illuminant, and filter-set; the ΔE_{ab}^* errors in the color-estimates of the 343 copier reflectances (from the simulated noisy scanner measurements using the optimal filters) were used to determine and tabulate the following: ΔE_{avg} , the average ΔE_{ab}^* value of the set; ΔE_{max} , the maximum ΔE_{ab}^* in the set; $\Delta E_{ab}^* \geq 3$, the number of errors with a ΔE_{ab}^* greater than three. The number of ΔE_{ab}^* values greater than three are given since such values are perceptually noticeable by the average observer.

A comparison of Table 1 with the corresponding table for the sub-optimal nonnegative filters presented in [3] reinforces the conclusions drawn from the graphs in Fig 1. In almost all comparisons, the optimal nonnegative filters offer significant improvements over their suboptimal counterparts, with the largest improvements for low SNRs and for filter sets with larger number of filters. Both the graph and the table indicate that at all simulated SNRs, going from three to four filters offers the most significant decrease in the average ΔE_{ab}^* error, and the improvement obtained upon using more than 4 filters is incremental. Hence, it is desirable to use a four-channel scanner and four-tuples for obtaining multi-illuminant color information. Vrhel *et al.* [3] first arrived at this conclusion, which is strengthened by these new results.

In addition to the feasibility requirement embodied in the nonnegativity constraint, it is desirable that the filter-set \mathbf{G} be readily fabricable for use in a scanning device. The manufacturability of the sub-optimal 4-filter set from [3], using dichroic materials, was examined in [15], and fairly close approximations to the sub-optimal filter-sets were deemed producible. A similar study has not been performed for the optimal filter-sets determined in this paper. However, it is unlikely that there will be significant differences in manufacturability between the optimal and the sub-optimal filters. This claim is validated by the details of the fabrication procedure described in [15] and by the comparison of the optimal and sub-optimal nonnegative 4-filter sets at 30 dB SNR shown in Fig. 2.

5 Conclusion

Optimal nonnegative color-scanning filters (for multi-illuminant color correction) designed in this paper were shown to offer significant improvements in color recording accuracy in comparison with a sub-optimal scheme reported in earlier literature. The simulation results further reinforced the conclusion in [3] that for multi-illuminant color-recording the use of four-tuples is desirable, instead of the tristimuli currently used.

6 Acknowledgment

A grant of supercomputer time from the North Carolina Supercomputing Center, RTP, NC is gratefully acknowledged.

References

- [1] M. J. Vrhel and H. J. Trussell, “Filter considerations in color correction,” *IEEE Trans. Image Proc.*, vol. 3, no. 2, pp. 147–161, Mar. 1994.
- [2] M. Wolski, J. P. Allebach, C. A. Bouman, and E. Walowit, “Optimization of sensor response functions for colorimetry of reflective and emissive objects,” *IEEE Trans. Image Proc.*, vol. 5, no. 3, pp. 507–517, Mar. 1996.
- [3] M. J. Vrhel and H. J. Trussell, “Optimal color filters in the presence of noise,” *IEEE Trans. Image Proc.*, vol. 4, no. 6, pp. 814–823, Jun. 1995.
- [4] G. Sharma and H. J. Trussell, “Digital color imaging,” *IEEE Trans. Image Proc.*, vol. 6, no. 7, Jul. 1997.
- [5] CIE, “Colorimetry,” CIE Publication No. 15.2, Central Bureau of the CIE, Vienna, 1986.
- [6] G. Sharma and H. J. Trussell, “Figures of merit for color scanners,” *IEEE Trans. Image Proc.*, vol. 6, no. 7, Jul. 1997.
- [7] W. K. Pratt, *Digital Image Processing*, John Wiley & Sons, New York, second edition, 1991.
- [8] H. Haneishi, T. Hirao, A. Shimazu, and Y. Mikaye, “Colorimetric precision in scanner calibration using matrices,” in *Proc. Third IS&T/SID Color Imaging Conference: Color Science, Systems and Applications*, Nov. 1995, pp. 106–108.
- [9] Jan R. Magnus and Heinz Neudecker, *Matrix Differential Calculus with Applications in Statistics and Econometrics*, Wiley, 1988.
- [10] David G. Luenberger, *Linear and Nonlinear Programming*, Addison Wesley, Reading, MA, second edition, 1989.
- [11] J. Phillips, *The NAG Library : a beginner’s guide*, Clarendon Press, New York, NY, 1986.
- [12] G. Wyszecki and W. S. Stiles, *Color Science: Concepts and Methods, Quantitative Data and Formulae*, John Wiley & Sons, Inc., New York, second edition, 1982.

- [13] G. Sharma, *Color scanner characterization, performance evaluation, and design*, Ph. D. dissertation, North Carolina State University, Aug. 1996.
- [14] M. J. Vrhel, *Mathematical Methods of Color Correction*, Ph. D. dissertation, North Carolina State University, May 1993.
- [15] M. J. Vrhel, H. J. Trussell, and J. Bosch, “Design and realization of optimal color filters for multi-illuminant color correction,” *J. Electronic Imaging*, vol. 4, no. 1, pp. 6–14, Jan. 1995.

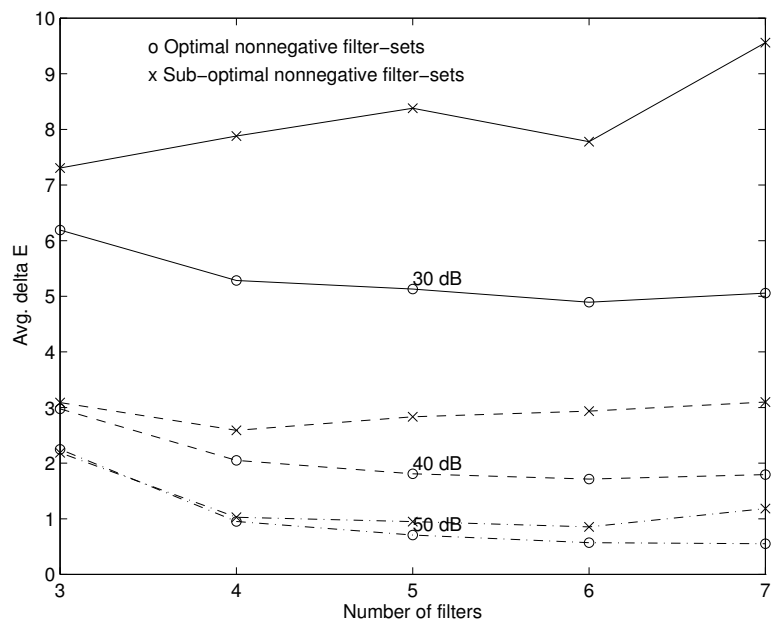
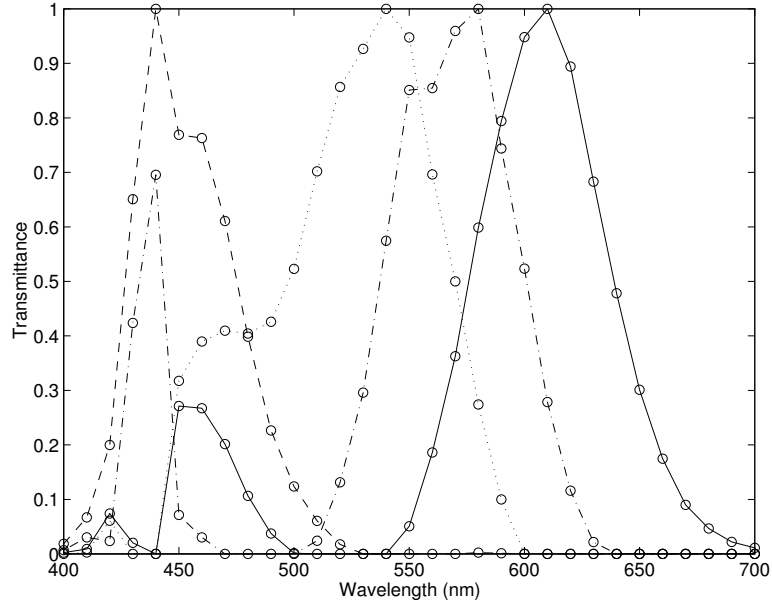
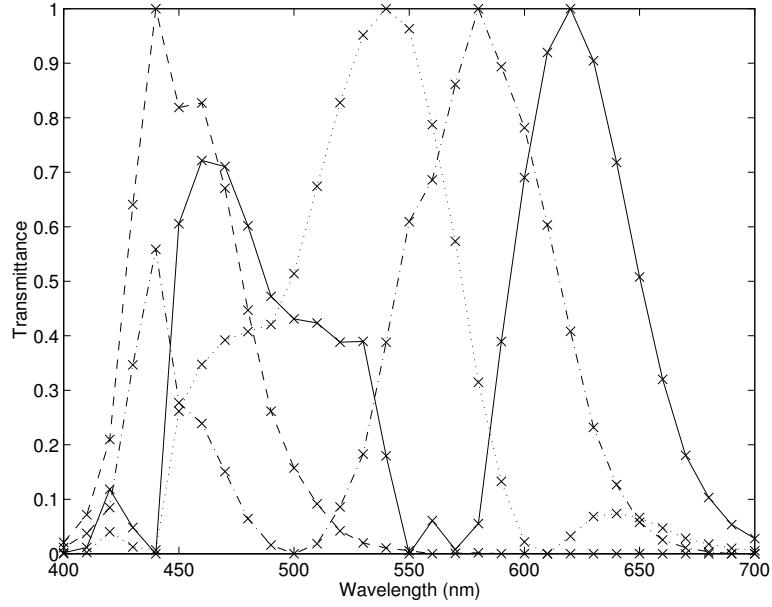


Figure 1: Performance comparison of optimal and sub-optimal filter sets.



(a)



(b)

Figure 2: (a) Optimal and (b) sub-optimal 4-filter sets at 30 dB SNR.

SNR		30			35			40			45			50		
No.	Stat- istic	Illuminant			Illuminant			Illuminant			Illuminant			Illuminant		
Filt.		D65	A	F2	D65	A	F2	D65	A	F2	D65	A	F2	D65	A	F2
3	ΔE_{avg}	5.88	6.39	6.31	3.43	4.58	4.16	2.28	3.60	3.04	1.78	3.06	2.53	1.55	2.90	2.30
	ΔE_{max}	27.10	26.98	35.20	20.08	21.94	42.83	12.75	16.14	28.41	10.58	11.80	15.10	8.78	11.50	14.89
	$\Delta E \geq 3$	237	250	245	147	198	176	80	150	102	52	132	88	38	126	72
4	ΔE_{avg}	5.17	5.40	5.29	3.16	3.29	3.31	1.93	2.04	2.18	1.17	1.29	1.53	0.75	0.89	1.22
	ΔE_{max}	24.33	36.03	29.37	14.11	15.46	14.55	8.74	9.42	9.76	5.57	5.82	6.34	3.49	3.71	4.41
	$\Delta E \geq 3$	216	228	225	146	149	144	55	67	77	21	19	35	3	3	15
5	ΔE_{avg}	5.09	5.26	5.04	2.94	3.06	2.97	1.75	1.82	1.86	1.06	1.10	1.22	0.64	0.62	0.87
	ΔE_{max}	23.72	24.99	22.86	13.83	15.48	13.86	7.90	9.72	9.01	4.79	4.91	6.11	3.93	3.44	4.43
	$\Delta E \geq 3$	218	226	216	133	138	136	49	61	57	10	11	14	2	1	3
6	ΔE_{avg}	4.81	5.11	4.76	2.69	2.88	2.94	1.66	1.71	1.77	0.93	0.99	0.98	0.52	0.56	0.63
	ΔE_{max}	22.67	26.08	23.74	13.66	12.71	14.22	9.07	7.44	7.18	4.20	4.93	4.37	2.48	2.39	2.96
	$\Delta E \geq 3$	215	219	214	107	121	131	44	43	55	5	11	7	0	0	0
7	ΔE_{avg}	4.93	5.15	5.10	2.80	2.93	2.94	1.69	1.96	1.74	0.90	0.98	0.98	0.52	0.56	0.57
	ΔE_{max}	27.68	31.84	28.06	14.69	14.50	16.10	8.08	10.04	10.98	3.67	5.00	5.42	2.10	2.89	2.99
	$\Delta E \geq 3$	224	219	224	117	118	119	48	65	53	4	6	5	0	0	0

Table 1: ΔE_{ab}^* Error Statistics for optimal nonnegative filter-sets.

List of Figures

1	Performance comparison of optimal and sub-optimal filter sets.	10
2	(a) Optimal and (b) sub-optimal 4-filter sets at 30 dB SNR.	11

List of Tables

1	ΔE_{ab}^* Error Statistics for optimal nonnegative filter-sets.	12
---	---	----